Published in final edited form as:
Glia. 2007 March ; 55(4): 400–411.

INSULIN-LIKE GROWTH FACTOR TYPE 1 RECEPTOR SIGNALING IN THE CELLS OF OLIGODENDROCYTE LINEAGE IS REQUIRED FOR NORMAL *IN VIVO* OLIGODENDROCYTE DEVELOPMENT AND MYELINATION

Martha Zeger[1], **Greg Popken**[1], **Jihui Zhang**[1], **Shouhong Xuan**[2], **Q. Richard Lu**[3,*], **Markus H. Schwab**[4], **Klaus-Armin Nave**[4], **David Rowitch**[3,#], **A. Joseph D'Ercole**[1], and **Ping Ye**[1]

1 *Dept of Pediatrics, University of North Carolina at Chapel Hill, Chapel Hill, NC*

2 *Dept of Genetics and Development, Columbia University, New York, New York*

3 *Dana-Farber Cancer Institute, Harvard University, Boston, MA*

4 *Dept of Neurogenetics, Max Planck Institute of Experimental Medicine, Germany*

Abstract

Insulin-like growth factor-I (IGF-I) has been shown to be a potent agent in promoting the growth and differentiation of oligodendrocyte precursors, and in stimulating myelination during development and following injury. To definitively determine whether IGF-I acts directly on the cells of oligodendrocyte lineage, we generated lines of mice in which the type 1 IGF receptor gene (*igf1r*) was conditionally ablated either in Olig1 or proteolipid protein expressing cells (termed $IGF1R^{pre\text{-}oligo\text{-}ko}$ and $IGF1R^{oligo\text{-}ko}$ mice, respectively). Compared to wild type mice, $IGF1R^{pre\text{-}oligo\text{-}ko}$ mice had a decreased volume (by 35% to 55 %) and cell number (by 54% to 70%) in the corpus callosum (CC) and anterior commissure at 2 and 6 weeks of age, respectively. $IGF1R^{oligo\text{-}ko}$ mice by 25 weeks of age also showed reductions, albeit less marked, in CC volume and cell number. Unlike astrocytes, the percentage of $NG2^+$ oligodendrocyte precursors was decreased by ~13% in 2-week-old $IGF1R^{pre\text{-}oligo\text{-}ko}$ mice, while the percentage of $CC1^+$ mature oligodendrocytes was decreased by ~24% in 6-week-old $IGF1R^{pre\text{-}oligo\text{-}ko}$ mice and ~25% in 25-week-old $IGF1R^{oligo\text{-}ko}$ mice. The reduction in these cells is apparently a result of decreased proliferation and increased apoptosis. These results indicate that IGF-I directly affects oligodendrocytes and myelination *in vivo* via IGF1R, and that IGF1R signaling in the cells of oligodendrocyte lineage is required for normal oligodendrocyte development and myelination. These data also provide a fundamental basis for developing strategies with the potential to target IGF-IGF1R signaling pathways in oligodendrocyte lineage cells for the treatment of demyelinating disorders.

Keywords

IGF-I; IGF1R; Olig1; PLP; MBP; mutant mice; oligodendrocyte precursors

Correspondence should be addressed to Dr. Ping Ye, Department of Pediatrics, CB# 7039, The University of North Carolina at Chapel Hill, Chapel Hill, NC 27599-7039, Tel: (919) 966-4435, Fax: (919) 966-2423, E-mail: ping_ye@med.unc.edu.
*Current address: Center for Developmental Biology, University of Texas Southwestern Medical Center, Dallas, TX
#Current address: Department of Pediatrics and Program in Stem Cell Biology, UCSF, San Francisco, CA

INTRODUCTION

A significant amount of experimental data has provided compelling evidence that insulin-like growth factor-I (IGF-I) has an important role in the growth and survival of oligodendrocyte lineage cells, as well as myelination, in the central nervous system (CNS) during development and following injury. During development IGF-I and its receptor, the type I IGF receptor (IGF1R), are widely expressed in the CNS. The peak expression of each often occurs in spatial coordination with rapid neural growth (see reviews by Anlar et al., 1999; Bondy and Cheng, 2004; D'Ercole et al., 1996; McMorris et al., 1993). Using transgenic (Tg) technology we (Mason et al., 2000;Ye et al., 1995a; 1995b;Ye et al., 2000) and others (Carson et al., 1993; Luzi et al., 2004; Mason et al., 2003) have demonstrated that brain IGF-I overexpression in Tg mice promotes myelination during development and protects against damage. Conversely, ablation of IGF-I expression (Ye et al., 2002) or inhibition of IGF-I bioactivity by ectopic expression of IGF binding protein (IGFBP)-1 in developing brain (Ni et al., 1997; Ye et al., 1995a; 1995b) decreases myelination. Consistent with these observations in mutant mice, IGF-I has been reported to promote oligodendrocyte development in the hippocampus (Hsieh et al., 2004) and to reduce cell death induced by axon transection in optic nerve (Barres et al., 1993) when delivered by IGF-I expression vectors or overexpressing cells, respectively.

While the studies mentioned above demonstrate IGF-I actions on oligodendrocyte lineage cells during development and following injury, there is as yet no *in vivo* experimental evidence showing a direct interaction of IGF-I and cells of the oligodendrocyte lineage. A study by Chen et al. (1998) suggested that IGF-I actions on oligodendrocytes and myelination *in vivo* are indirect. They (Cheng et al., 1998) showed that young adult mice with an IGF-I null mutation (IGF-I KO mice) and their littermate controls have an identical concentration of several myelin-specific proteins and a similar ratio of oligodendrocyte to projection neuron number, despite an ~25% reduction in myelin-associated galactocerebroside and sulfatide in the IGF-I KO mice. Because neurons, astrocytes and other neural cells also express the IGF1R, it was possible that IGF-I indirectly influenced oligodendrocyte lineage cells and myelination by acting on neurons and/or astrocytes, which in turn directed promoted oligodendrocyte lineage development and myelination.

A precise understanding IGF-I *in vivo* actions is critical to the development of therapeutic strategies using IGF-I, likely together with other agents, in treatment of demyelinating disorders. We set out, therefore, to definitively determine whether IGF-I acts directly on the cells of oligodendrocyte lineage *in vivo* by generating mutant mice in which the function of the IGF1R was specifically ablated in the cells of oligodendrocyte lineage, using a Cre/loxP strategy and mice carrying a Cre transgene driven either by Olig1 or PLP gene regulatory regions. Cre expression predominates in early oligodendrocyte precursors in the former Olig1-driven Tg mice and peaks in maturing oligodendrocytes in the later PLP-driven Tg mice. Here we provide evidence that IGF affects oligodendrocyte development and myelination *in vivo* by directly interacting with IGF1R, and that IGF1R signaling in the cells of oligodendrocyte lineage is required for normal oligodendrocyte development and myelination.

MATERIALS AND METHODS

Generation of IGF1R$^{pre\text{-}oligo\text{-}ko}$ and IGF1R$^{oligo\text{-}ko}$ mice

Mice with ablated IGF1R expression in Olig1-expressing oligodendrocyte precursors, termed IGF1R$^{pre\text{-}oligo\text{-}ko}$ mice, or in PLP-expressing oligodendrocytes, termed IGF1R$^{oligo\text{-}ko}$ mice, were generated by breeding mutant mice carrying a loxed exon 3 of the *igf1r* gene (IGF1R$^{Lox/Lox}$ mice) with mice carrying a Cre transgene driven by either Olig1 (Cre^{Olig1} Tg mice) or PLP (Cre^{PLP} Tg mice) gene regulatory regions, respectively. Generation and characterization of IGF1R$^{Lox/Lox}$ mutant (Xuan et al., 2002) and Cre^{Olig1} Tg (Lu et al.,

2002) mice have been described in detail elsewhere. Cre^{PLP} Tg mice were generated using a Cre transgene driven by a rodent PLP promoter (Genoud, 2002; Goebbels, Schwab and Nave unpublished data). The mutant mice were genotyped using Southern blot hybridization and/or PCR analysis of tail DNA. Before experimentation all mutant breeder mice (i.e., Cre^{Olig1} Tg, Cre^{PLP} Tg and $IGF1R^{Lox/Lox}$ mice) were crossbred with C57B/6L mice for >6 generations to obtain a similar genomic background. All procedures used were consistent with the guidelines of National Institutes of Health and approved by the institutional review committees of the University of North Carolina at Chapel Hill, Harvard University, Columbia University, USA, and Max Planck Institute of Experimental Medicine, Germany.

Southern Blot Hybridization Analysis

Aliquots of genomic DNA (12-15 og) were digested with the restriction enzyme BamHI or Kpn I, fractionated on agarose gels, transferred onto a nylon membrane. The membranes were hybridized with ^{32}P-labeled single stranded DNA probes generated using the pGEM 5Z or 7Z plasmid containing a fragment of *igf1r* DNA as template (Mason et al., 2003; Xuan et al., 2002), as previously reported (Ye et al., 1995a).

Western Blot Analysis

Protein was extracted as previously described (Klugmann et al., 1997), and stored at −80°C until use. Aliquots of 30 - 60 μg protein were separated on polyacrylamide gels and transferred onto PVDF membranes. Specific proteins of interest were detected using their specific antibodies: MBP (1:1,500, Chemicon Internationals, Temecula, CA); 2',3'-cyclic nucleotide 3'-phosphodiesterase (CNP, 1:500; Chemicon); glial fibrillary acidic protein (GFAP, 1:3,000, Chemicon); IGF1R β-subunit (1:1,500, Santa Cruz Biotechnology, Santa Cruz, CA); and β-actin (1:5,000, Sigma, St. Louis, MO). The abundance of specific proteins was quantified using a computer-assisted image analysis system (Image-Pro, Media Cybermetics, Silver Spring, MD). To insure the equal loading and accuracy of changes in protein abundance, the protein levels were normalized to ß-actin abundance. The abundance of ß-actin closely paralleled the amount of total protein loaded.

Immunohistochemical Staining

After fixation with cold 4% paraformaldehyde in phosphate-buffered saline (PBS) brains were sagittally sliced at the midline and paraffin-embedded. Near midline sagittal sections (at a thickness of 6 om) of right hemispheres were subjected to immunostaining with an antibody specific for CNP (1:1,000), proteolipid protein (PLP, 1:500, Chemicon), MBP (1:800), or neurofilament heavy chain subunit (NF-H, 1:500, Chemicon). Antibody-antigen complexes were detected using an ABC kit (Vector Laboratories, Burlingame, CA) and visualized by incubation with DAB.

β-galactosidase (LacZ) Histochemistry

LacZ staining was performed using a modified method of Mercer et al. (1991). Briefly, after perfusion fixation with cold 2% paraformaldehyde and 0.2% glutaraldehyde in PBS, brains were sagittally sliced along the midline into blocks in thickness of 1- 3 mm, and further fixed in the same solution for 3 hr at 4°C. After extensive washing brain slices were subjected to LacZ staining. For LacZ and immunohistochemical double staining, LacZ stained tissues were either frozen or paraffin-embedded, sectioned (6 – 8 μm in thickness), and immunostained with an antibody specific for NG2 (1:100, a gift from Dr. Bill Stallcup, The Burnham Institute, La Jolla, CA), GFAP (1:200, Chemicon), NeuN (1:200), or GST-π (1:500, Medlabs, Dublin, Ireland). Antibody-antigen complexes were detected using an ABC kit and visualized by incubation with DAB.

Stereological Analysis of Anterior Commissure (AC), Corpus Callosum (CC), and Dentate Gyrus (DG)

Paraffin embedded left half brains were sagittally cut, and 3 - 4 sets of serial sections (12 μm in thickness) obtained. For AC and CC volume and cell number, one series of sections comprised of every 20th section was immunostained for NF-H and counterstained with hematoxylin, or was stained with hematoxylin and eosin. For DG volume and the number of granule neurons in dentate gyrus, another series also comprised of every 20th section was stained with Cresyl Violet. Assisted with Stereo Investigator software (Microbrightfield, Colchester, VT), the area of AC and CC in sections [corresponding to plates between number 55 and 143 and between 144 and 172, respectively, in the Altas Of The Mouse Brain And Spinal Cord (Sidman et al., 1971)] was measured. Similarly, the area of DG and granule cell layer in every 20th section was measured. The volume of AC, CC, DG, and granule cell layer was estimated using the formula: $\sum A \times T \times I \times 2$, where $\sum A$ = sum of area measured on each section, with T = section thickness, I = section intervals, and 2 accounts for 2 half brains. At least ten sampling points (sections) for each structure were used.

To estimate the total number of cells in each region, the cell density in each region was multiplied by its volume. To determine cell density in AC and CC, 2 - 4 stained sections from each brain (see above) were randomly selected, and cell nuclei within delineated AC and CC areas were counted. In each section the cell density in each brain region was calculated by dividing the regional cell count by its respective volume, and then the regional cell density of each brain was obtained by averaging the cell density in each section. The total number of DG granule neurons was estimated using the optic dissector method. To correct potential counting bias due to difference in cell size and nuclear splitting among mice, cell nuclear volume (>200 in each brain) was measured and a correction was performed, using Abercrombie's method (Abercrombie, 1946).

Quantification of CC1$^+$ Oligodendrocytes, NG2$^+$ Oligodendrocyte Precursors, and GFAP$^+$ Astrocytes

Fresh frozen brains were sagittally sectioned at the thickness of 8 om on a cryostat. Two sections (at least 50 μm apart to avoid counting the same cells twice) were subjected to immunostaining with CC1 (1:50, Oncogene Research Products, CA), NG2 (1:200), Ki67 (1:500, Chemicon) or GFAP (1:200, Chemicon) antibodies. For GFAP$^+$ astrocytes in adult mutant mice, paraffin-embedded sections also were studied. Antibody-antigen complexes were detected using either an Alexa Fluor 488-conjugated anti-rabbit (Invitrogen, Carlsbad, CA) or a Cy3-conjugated anti-mouse (Jackson ImmunoResearch Laboratories, West Grove, PA) secondary antibody. Cell nuclei were counterstained with nuclear dye 4,6-diamidine-2'-phenylindole dihydrochloride (DAPI, Invitrogen). Immuno-labeled cells each with a clear nucleus (>400 cells in each section) were scored on the digitally captured images. The number of NG2$^+$, CC1$^+$, and GFAP$^+$ cells was calculated as the percentage of the total number of cells judged by nuclei. The nuclear volume of NG2$^+$, CC1$^+$, and GFAP$^+$ cells (~200 cells for each cell type in each brain) was measured, using the nucleator method and Stereo Investigator software. No significant difference in nuclear volume was observed between control and mutant mice, therefore, no correction was required.

Terminal Uridine Nucleic End Labeling (TUNEL)

TUNEL was performed using an *In Situ* Cell Death Detection Kit (Roche Applied Science, Indianapolis, IN) following the manufacturer's protocol; then paraffin-embedded or fresh-frozen near mid-sagittal sections were double-stained with either a mouse anti-GFAP antibody (1:500, Chemicon), NG2 or Iba-1 antibody (1:200, Wako Chemicals, Richmond, VA), followed by a Cy3 or an Alexa Fluor 594 conjugated secondary antibody, and DAPI. Labeled cells (>880) in each section were scored on the digitally captured images.

Statistics

Student-*t* test was used with the assistance of software SigmaStat for Windows (SPSS, Inc., Chicago, IL).

RESULTS

Oligodendrocyte precursors specific expression of the Cre^{Olig1} transgene has been previously reported (Lu et al., 2002). Data from one of our laboratories also show that the Cre^{PLP} transgene is specifically expressed in the cells of oligodendrocyte lineage, and the tempo-spatial expression pattern correlates closely with that of endogenous PLP (Goebbels, Schwab and Nave, unpublished data). Cre-mediated deletion of E3 of the *igf1r* gene in the brains of developing and adult $IGF1R^{pre\text{-}oligo\text{-}ko}$ and $IGF1R^{oligo\text{-}ko}$ mice was confirmed using Southern blot analysis of brain genomic DNA and RT-PCR of brain mRNA (Figure 1). Excision of E3 results in a deletion of most of the IGF-I binding domain coding region and a reading frame-shift mutation thereafter in the *igf1r* gene. Using an antibody specific for IGF1R β subunit (IGF1Rβ), Western immunoblot analysis of brains of $IGF1R^{pre\text{-}oligo\text{-}ko}$ mice at postnatal day 0 (a time approximately at the peak of IGF1R expression (Werner et al., 1989) demonstrated that IGF1R abundance was decreased by ~2 fold, as compared to wild type (WT) controls.

Genotyping of postnatal mice showed the occurrence of $IGF1R^{pre\text{-}oligo\text{-}ko}$ and $IGF1R^{oligo\text{-}ko}$ follows Mandel's distribution, i.e., ~25% were $IGF1R^{pre\text{-}oligo\text{-}ko}$ or $IGF1R^{oligo\text{-}ko}$ mice, when $IGF1R^{Lox/Lox}$ mice were bred with $Cre^{Olig1}/IGF1R^{Lox/Wt}$ mice or $Cre^{PLP}/IGF1R^{Lox/Wt}$ mice, respectively. These findings indicate that there is no prenatal lethality. Postnatal growth of both $IGF1R^{pre\text{-}oligo\text{-}ko}$ and $IGF1R^{oligo\text{-}ko}$ mice also was apparently normal, albeit that their body weights tended to be lighter than that of their littermates (data not shown).

To compare the expression pattern of the Cre^{Olig1} and Cre^{PLP} transgenes and their capacity to mediate DNA recombination during development, Cre^{Olig1} and Cre^{PLP} Tg mice were bred with $lacZ^{actin\text{-}stop}$ Tg mice which carry a β-galactosidase (LacZ) reporter transgene linked to a chicken actin promoter followed by a floxed "stop" DNA sequence (Araki et al, 1995). Deletion of the "stop" DNA sequence mediated by Cre leads to activation and expression of the LacZ reporter gene. Thus, the effects of Cre^{Olig1} and Cre^{PLP} gene expression in double Tg mice, i.e. $Cre^{Olig1}/lacZ^{actin\text{-}stop}$ and $Cre^{PLP}/lacZ^{actin\text{-}stop}$ Tg mice, can be determined using LacZ histochemical staining. In Cre^{Olig1} Tg mice abundant LacZ staining was observed throughout most brain regions, especially in white matter, at the first week of postnatal life, a time when few precursors have developed into mature oligodendrocytes in forebrain (Figure 2**).** Sparse motor neurons in brainstem (e.g., in facial nuclei), as well as Purkinje cells in cerebellum, however, also were positive for both LacZ and NeuN (data not shown). These findings are consistent with predominant Cre^{Olig1} expression in oligodendrocyte precursors and pre-mature oligodendrocytes, as reported by Lu et al (2002), as well as with the expression of the endogenous Olig1 gene in the brains of mice (Lu et al., 2000) and humans (Jakovcevski and Zecevic, 2005).

In contrast, LacZ expression was nearly undetectable in 1-week-old Cre^{PLP} Tg mice. By the second week of life LacZ expression in Cre^{PLP} Tg mice was readily seen in the brain stem, CB and diencephalon (Figure 2). With increasing age LacZ staining was significantly increased in Cre^{PLP} Tg mice (Figure 2). To further confirm cell specific expression of Cre^{PLP} transgene, LacZ stained brain sections derived from 4-week-old $Cre^{PLP}/lacZ^{actin\text{-}stop}$ Tg mice were double-stained with antibody specific for neural cell markers. As Figure 2, panel B shows, intense LacZ staining co-localized with the mature oligodendrocyte marker GST-π, but not with GFAP, an astrocyte marker, or NeuN, a neuron marker (except for cerebellar Purkinje cells that were positive for LacZ). In addition, little LacZ and NG2 co-localization was observed in Cre^{PLP} Tg mice (Figure 2). These data are consistent with previous data from one of our

laboratories (Goebbels, Schwab and Nave, unpublished data), and strongly indicate that Cre^{PLP} transgene expression, and the DNA recombination it mediates, predominately occurs in mature oligodendrocytes.

While there was no apparent abnormality in their body growth, the brain growth of $IGF1R^{pre\text{-}oligo\text{-}ko}$ mice was retarded (Figure 3, panel A). Compared to WT mice, the brain weightsof homozygous $IGF1R^{pre\text{-}oligo\text{-}ko}$ mice were significantly reduced, being ~92, ~88 and ~82% of WT controls at 1, 2 and 6 weeks of their postnatal life, respectively. $IGF1R^{oligo\text{-}ko}$ mice also exhibited a decreased brain weight. Compared to $IGF1R^{pre\text{-}oligo\text{-}ko}$ mice, the reduction occurred much later, being first observed at 3 weeks of age, although not statistically significant (Figure 3, panel B). When brain growth was analyzed as brain to body weight ratios, the developmental patterns of brain growth retardation observed in each line of mutant mice was nearly identical to that when only brain weight was analyzed (data not show). WT mice and the mice carrying Cre transgene and $IGF1R^{Lox}$ mutation exhibited no apparent difference in brain growth, nor did they exhibit any apparent morphological abnormalities. Data from these latter mice, therefore, were grouped for analysis, hereafter termed control mice.

To test whether blunting of IGF-I expression during early development affects myelination, we first immunohistochemically assessed the abundance of three major myelin-specific proteins, i.e., PLP, MBP and CNP, in the developing brains of $IGF1R^{pre\text{-}oligo\text{-}ko}$ and $IGF1R^{oligo\text{-}ko}$ mice. Compared to their littermate controls, both $IGF1R^{pre\text{-}oligo\text{-}ko}$ and $IGF1R^{oligo\text{-}ko}$ mice exhibited a marked reduction in the intensity of immunostaining. Representative photomicrographs of brain PLP and MBP immunostaining in developing and adult $IGF1R^{pre\text{-}oligo\text{-}ko}$ and $IGF1R^{oligo\text{-}ko}$ mice, as well as their littermate controls, are shown in Figures 4 and 5, respectively. Compared to their 2-week-old littermate controls that exhibit ample yellowish-brown PLP immunostaining in CTX (Figure 4, panel A) and bundles of PLP positive fibers in the CB (Figure 4, panel C), 2-week-old $IGF1R^{pre\text{-}oligo\text{-}ko}$ mice exhibited a marked reduction in PLP immunostaining in these regions (Figure 4, panels B and D). In contrast, immunostaining for heavy-chain neurofilament (NF-H) did not show significant differences between $IGF1R^{pre\text{-}oligo\text{-}ko}$ and control mice (Figure 4, panels G and H). During the next several weeks the intensity of PLP immunoreactivity increased significantly in all brain regions of both $IGF1R^{pre\text{-}oligo\text{-}ko}$ and control mice. PLP immunoreactivity in $IGF1R^{pre\text{-}oligo\text{-}ko}$ mice (Figures 4, panel F), however, remained significantly reduced, compared to control mice (Figures 4, panel E). Immunostaining of MBP and CNP in $IGF1R^{pre\text{-}oligo\text{-}ko}$ mice was reduced in a similar pattern during development (data not shown).

$IGF1R^{oligo\text{-}ko}$ also exhibited a decrease in immunostaining intensity for myelin-specific proteins (Figure 5). Compared with $IGF1R^{pre\text{-}oligo\text{-}ko}$ mice, however, the reduction in myelin protein immunoreactivity occurred much later during development and was not evident until 3–4 weeks of postnatal life (Figure 5, panel B). The myelin protein immunostaining in $IGF1R^{oligo\text{-}ko}$ mice was further reduced at 25 week of age (Figure 5, panel D).

Next we used Western immunoblot analysis to quantify the changes in CTX MBP and CNP protein abundance. At 6 weeks of age, 4 major MBP bands (~14 kDa, ~17 kDa, ~18 kDa and ~21 kDa) and a single CNP band (~50 kDa) are readily detected (Figure 6). When compared to littermate controls, the abundance of both MBP (when the abundance of all 4 MBP bands is combined for quantification) and CNP proteins in $IGF1R^{pre\text{-}oligo\text{-}ko}$ mice was decreased by ~40% and ~70%, respectively (Figure 6, panels A and C), while GFAP abundance in $IGF1R^{pre\text{-}oligo\text{-}ko}$ mice was only moderately reduced and the change did not meet statistical significance. Six-week-old $IGF1R^{oligo\text{-}ko}$ mice also exhibited 20 – 30 % reduction in MBP and CNP abundance in CTX (Figure 6, panels B and D).

The impact of deletion of IGF1R signaling in the growth of glial cells was determined by comparing the number of cells in CC and AC, two myelin-rich regions that contain primarily glial cells (oligodendrocyte precursors, mature oligodendrocytes, astrocytes, and microglia) and neuronal axons. Photomicrographs of 2-week-old IGF1R$^{pre\text{-}oligo\text{-}ko}$ mice (Figure 7, panels C and D) revealed an apparent decrease in CC and AC size and the cell density in these two regions, compared to littermate controls (Figure 7, panels A and B). Further quantitative analysis showed that in IGF1R$^{pre\text{-}oligo\text{-}ko}$ mice the volumes of CC and AC were decreased by ~35% to ~55%, while the cell density was reduced by ~27% to ~35% (Figure 7, panel E). As a result there were significant reductions in the total number of cells in the CC (by~54%), the anterior portion of the AC (by ~70%), and the posterior portion of the AC (~60%). In 6-week-old IGF1R$^{pre\text{-}oligo\text{-}ko}$ mice the CC volume, cell density and total cell number remained reduced by ~35%, ~27% and ~56%, respectively (Figure 7, panel E). IGF1R$^{oligo\text{-}ko}$ mice at 25-weeks of age also had significant decreases in CC volume, cell density and total number of cells (Table 1).

To further assess the cellular growth of the oligodendrocyte lineage in IGF1R$^{pre\text{-}oligo\text{-}ko}$ mice, the percentage of NG2$^+$ oligodendrocyte precursors, proliferating NG2$^+$ oligodendrocyte precursors, and CC1$^+$ mature oligodendrocytes in CC was determined. Compared to their littermate controls, the percentage of NG2$^+$ oligodendrocyte precursors in IGF1R$^{pre\text{-}oligo\text{-}ko}$ mice was decreased by ~13% at 2 weeks of age and was further reduced by ~17% at 6 weeks of age (Figure 8, panel C). At 2 weeks of age NG2 cells represented 19.40 ± 0.13 % of all CC cells in IGF1R$^{pre\text{-}oligo\text{-}ko}$ mice, compared to 22.61 ± 0.22 % (P<0.05) in controls, while at 6 weeks of age they represented 5.64 ± 0.07 % of total CC cells in mutant mice compared to 6.76 ± 0.35 % (P<0.05) in controls. In line with the changes in NG2$^+$ oligodendrocyte precursor, the percentage of proliferating NG2$^+$ oligodendrocyte precursors, as identified by double-immunolabeling with NG2 and Ki67, a protein that is expressed in the G1, G2 and M phases of cycling cells, was significantly reduced by ~30% in IGF1R$^{pre\text{-}oligo\text{-}ko}$ mice at 2 weeks of age (Figure 8). Examination of 1-week-old IGF1R$^{pre\text{-}oligo\text{-}ko}$ mice also showed a similar reduction in the number of NG2 and Ki67 double-labeled cells (data not shown).

Consistent with changes in the number of NG2$^+$ oligodendrocyte precursors, the number of CC1$^+$ mature oligodendrocytes was also significantly reduced in the CC of 6-week-old IGF1R$^{pre\text{-}oligo\text{-}ko}$ mice (Figure 8, panels B and C). Compared to controls, the percentage of CC1$^+$ mature oligodendrocytes was reduced by ~24% in IGF1R$^{pre\text{-}oligo\text{-}ko}$ mice (Figure 8). Similarly, in the CC of 25-week-old IGF1R$^{oligo\text{-}ko}$ mice the number of CC1$^+$ mature oligodendrocytes was reduced by ~24% (Figure 9). In a single experiment of PLP *in situ* hybridization, 6-week-old IGF1R$^{oligo\text{-}ko}$ mice also showed a markedly decreased number of PLP mRNA$^+$ oligodendrocytes in CC (data not shown).

To examine whether other cell types were affected, astrocytes in CC and neurons in the granule layer of dentate gyrus were determined. We selected dentate gyrus to facilitate our counting of neuronal number because its cellular architecture is well defined and granule neurons constitute more than 95% of its cells. In contrast to the marked decreases in total number of glial cells and percentage of NG2$^+$ oligodendrocyte precursors, the percentage of astrocytes in the CC, as judged by GFAP immunostaining, was increased by ~15% in 2-week-old IGF1R$^{pre\text{-}oligo\text{-}ko}$ mice and by ~25% in 6-week-old IGF1R$^{pre\text{-}oligo\text{-}ko}$ mice (Figure 8, panel C). Similarly, the percentage of GFAP$^+$ astrocytes was increased by ~25% in the CC of 25-week-old IGF1R$^{oligo\text{-}ko}$ mice (Figure 9). As with reduced brain and CC size (Figures 3 and 7), the volume of both dentate gyrus and granule neuron layer was reduced by ~27% in 2-week-old IGF1R$^{pre\text{-}oligo\text{-}ko}$ mice. When compared to littermate control mice, the total number of dentate gyrus granule neurons was only moderately reduced (by ~10%), and the reduction did not meet statistical significance (Table 2).

To determine whether blunting IGF1R function impacts cell survival in IGF1R$^{pre\text{-}oligo\text{-}ko}$ mice and whether increased cell death contributes to the reduction in oligodendrocyte precursors in the CC of IGF1R$^{pre\text{-}oligo\text{-}ko}$ mice, we performed TUNEL labeling. Unlike the paws of a rat at age of embryonic day (E) 16, which undergoes substantial morphological remodeling and has abundant apoptotic cells (Figure 10, panel A), only a very small fraction of CC cells (~0.4%) were TUNEL positive in control mice at 2 weeks of age. This finding is consistent with the data of Barres et al.(Barres et al., 1992) who showed that rat optic nerve has ~0.2% apoptotic oligodendrocytes during the same development period. Double immunostaining with glial cell markers showed that TUNEL labeling did not co-localize with GFAP or Iba-1 immunostaining, and less than 8% TUNEL labeled cells were positive for NG2 immunostaining (Figure 10, panel A). The low abundance of TUNEL and NG2 immuno-labeled cells made it impossible to accurately perform detailed quantification. Nonetheless, when compared to their littermate controls, the number of apoptotic cells in the CC was increased by ~65% in 2-weeks-old IGF1R$^{pre\text{-}oligo\text{-}ko}$ mice and by ~37% in newborn mutant mice, respectively (Figure 10, panel B).

DISCUSSION

This study evaluates the direct *in vivo* actions of IGF-I mediated by the IGF1R on oligodendrocyte lineage cells and myelination, using two mutant mouse models. In one mutant mouse line IGF1R function is blunted in Olig1-expressing oligodendrocyte precursors (IGF1R$^{pre\text{-}oligo\text{-}ko}$ mice) and in the other it is blunted in PLP-expressing mature oligodendrocytes (IGF1R$^{oligo\text{-}ko}$ mice). We demonstrate that disrupting IGF-IGF1R signaling in oligodendrocyte precursors during early development results in significant reductions in: 1) the size of the brain, AC and CC, two myelin-rich regions, 2) the number of cells in the AC and CC, 3) the number of NG2^{+} oligodendrocyte precursors, and 4) the number of proliferating NG2^{+} oligodendrocyte precursors. Furthermore, we show that CC1^{+} mature oligodendrocytes and myelin-specific proteins CNP and MBP are markedly reduced in adult IGF1R$^{pre\text{-}oligo\text{-}ko}$ mice. In contrast, there is no or little change in the abundance of the astrocyte-specific protein GFAP and the neuron-specific protein NF, or in the number of granule neurons in these mice.

Similarly, IGF1R$^{oligo\text{-}ko}$ mice exhibit significant decreases in brain weight, AC and CC size and cell number, and CNP and MBP abundance. These reductions only become evident 3-4 weeks after birth, and are 2 to 3 weeks later than in IGF1R$^{pre\text{-}oligo\text{-}ko}$ mice. The time of the observed reduction in myelination in IGF1R$^{oligo\text{-}ko}$ mice is concurrent with the time of peak expression of the endogenous PLP gene and the Cre^{PLP} transgene, and this is several weeks later compared to the expression of the endogenous Olig1 gene and the Cre^{Olig1} transgene. Although low levels of the Cre^{PLP} transgene is likely expressed in the embryonic brain and in oligodendrocyte precursors, as is the case with the endogenous PLP gene (Spassky et al., 2000), our unpublished data and data obtained in this study clearly demonstrate that Cre^{PLP} transgene expression closely follows the pattern of endogenous PLP gene expression (Jordan et al., 1989; Milner et al., 1985; Shiota et al., 1989; Sorg et al., 1987; Ikenaka et al., 1992; also see review by Nave and Milner, 1989; Spassky et al., 2000), and the DNA recombination it mediates occurs predominately in myelinating oligodendrocytes during late postnatal development, resulting in a later reduction in myelination in IGF1R$^{oligo\text{-}ko}$ mice, as compared to IGF1R$^{pre\text{-}oligo\text{-}ko}$ mice. As with IGF1R$^{pre\text{-}oligo\text{-}ko}$ mice, we observed little or no change in the abundance of the astrocyte-specific protein GFAP, the neuron-specific protein NF, or the number of DG granule neurons in IGF1R$^{oligo\text{-}ko}$ mice. Each of these findings is consistent with the cellular specificity of the Cre transgene expression (Lu et al, 2002; Goebbels, Schwab and Nave, unpublished data; and this study) and the disruption of the IGF1R gene function. Taken together, our data strongly indicate that IGF directly and specifically affects oligodendrocytes and myelination *in vivo* through the IGF1R, and that IGF1R signaling in both oligodendrocyte

precursors and mature oligodendrocytes is required for normal oligodendrocyte development and myelination.

Previously Efstratiadis and associates (Baker et al., 1993; Liu et al., 1993; Louvi et al., 1997) used genetic methodology and definitively demonstrated that the IGF1R mediates most, if not all, of IGF-I and IGF-II actions. Although both murine IGF-I and IGF-II are expressed beginning in prenatal life, each exhibits a distinct expression pattern in the CNS. While IGF-II is expressed at a high level in most brain regions during embryonic development, its expression decreases with increasing age. By birth little IGF-II mRNA can be detected in mouse brain, with the exceptions of meninges and choroid plexuses (Ayer-LeLievre et al., 1991; see review by Popken et al., 2005). In contrast, brain IGF-I expression begins somewhat later in the embryo, reaches its peak expression during the first week of postnatal life, and remains at relative high levels throughout life (Bach MA et al., 1996;Bartlett et al., 1992;Bondy, 1991; Popken et al., 2005). It appears very likely, therefore, that deletion of IGF1R function mediated by the Cre^{Olig1} expression in $IGF1R^{pre\text{-}oligo\text{-}ko}$ mice blunts the signaling of both IGF-I and IGF-II in oligodendrocyte precursors, as well as in mature oligodendrocytes, during embryonic and early postnatal development. Because of a much later expression of the Cre^{PLP} transgene, it also seems likely that the Cre^{PLP}–mediated IGF1R mutation predominately blocks IGF-I action in the later developing and adult brain. These conclusions are supported by data from our previous studies and those of others showing: 1) oligodendrocytes and their precursors express IGF1R *in vivo* and *in vitro* (Bondy et al., 1990; Mason and Goldman, 2002; Masters et al., 1991; Saneto et al., 1988); and 2) addition of IGFs to cultures promotes proliferation, survival and/or maturation of oligodendrocyte lineage cells and stimulates myelin-associated protein gene expression and myelin production (Barres et al., 1992; McMorris et al., 1986; McMorris and Dubois-Dalcq, 1988; Mozell and McMorris, 1991; Saneto et al., 1988; Ye and D'Ercole, 1999).

We observed that the percentage of $NG2^+$ oligodendrocyte precursors and $CC1^+$ oligodendrocytes is only moderately decreased (by 15 to 24%) in the CC of 2- and 6-week-old $IGF1R^{pre\text{-}oligo\text{-}ko}$ mice. Because the total number of CC cells was reduced by ~54% and ~44% in 2-and 6-week-old $IGF1R^{pre\text{-}oligo\text{-}ko}$ mice, respectively, however, the total number of $NG2^+$ oligodendrocyte precursors is estimated to be reduced by ~60% and ~54% in the CC of $IGF1R^{pre\text{-}oligo\text{-}ko}$ mice at these ages. Similarly, it is estimated that total CC $CC1^+$ oligodendrocytes in adult $IGF1R^{pre\text{-}oligo\text{-}ko}$ mice is decreased by ~56%.

Reduction in the number of oligodendrocytes and their precursors in mice with blunted IGF1R appears to be due to a decreased proliferation of precursors and an increase in their apoptosis. In $IGF1R^{pre\text{-}oligo\text{-}ko}$ mice the number of proliferating $NG2^+$ oligodendrocyte precursors, as judged by double-immunolabeling with Ki67, a marker for cycling cells, is significantly reduced. These data are consistent with our previous *in vitro* data and those of others showing that IGF-I promotes proliferation of neural cells, including cultured $A2B5^+$ oligodendrocyte precursors (see review by Popken et al., 2005; Ye and D'Ercole, 2006). Our data also are in line with the data of Hodge et al. (2004), who showed that overexpressing IGF-I in the brains of transgenic embryos increases proliferation of neuronal progenitors by decreasing duration of the cell cycle and by increasing the percentage of daughter cells re-entering the cell cycle. In neuronal progenitors the decreased duration of the cell cycle induced by IGF-I results entirely from a shortened G1 phase (Hodge et al., 2004). Whether IGF-I also promotes cell cycle progression through G1 phase in oligodendrocyte precursors *in vivo*, however, remains to be determined. Nonetheless, our data strongly support a role for IGF-IGF1R signaling in the proliferation of oligodendrocyte precursors during early development.

An increase in the death of oligodendrocyte lineage cells also may contribute to the decreased number in oligodendrocytes and their precursors in these mutant mice. The number of apoptotic

cells was observed to be increased in IGF1R$^{pre\text{-}oligo\text{-}ko}$ mice. Only a small fraction of these apoptotic cells were immuno-positive for NG2, and we were unable to determine the identity of the remaining apoptotic cells using the astrocyte marker GFAP and microglia marker Iba-1. It is likely that dying apoptotic cells are removed rapidly and/or their antigenic marker(s) are lost, resulting in few cells capable of reacting to antibodies. The paucity of cells that are both positive for apoptotic and oligodendrocyte markers made it impossible for us to accurately determine the number of apoptotic oligodendrocyte lineage cells in these mutant mice. Nonetheless, the finding that the number of apoptotic cells was increased in the CC of IGF1R$^{pre\text{-}oligo\text{-}ko}$ mice suggests that IGF-IGF1R signaling promotes survival of glial cells in the developing CC.

While IGF1R$^{pre\text{-}oligo\text{-}ko}$ mice have a similar number of granule neurons, they also exhibit a decreased number of GFAP$^+$ cells in CC, in spite of a modest increase in their percentage of total cells. The latter results from the dramatic reduction in the total number of CC cells. Mice with ablated IGF1R specifically in PLP-expressing cells (IGF1R$^{oligo\text{-}ko}$ mice), on the other hand, exhibit a much less dramatic reduction in the number of CC cells (by ~29%) and GFAP$^+$ cells (by ~5%). The reason(s) that account for the reduction in GFAP$^+$ cells in IGF1R$^{pre\text{-}oligo\text{-}ko}$ mice remains to be further investigated, and is beyond the scope of the current study; however, we speculate that because oligodendrocytes/astrocytes may come from the same glial precursors (Herrera et al., 2001; Gregori et al., 2002; Rao et al., 1998), ablating IGF1R in Olig1 expressing oligodendrocyte/astrocyte precursors blunts both oligodendrocyte and astrocyte precursor development. Alternatively, ablation of IGF1R in the cells of oligodendrocyte lineage indirectly reduces GFAP$^+$ cells in some other way(s), such as compromising oligodendrocyte-axon interactions that in turn lead to decreased proliferation and recruitment of astrocytes by axons.

In summary, we have demonstrated that blunting IGF-IGF1R signaling in oligodendrocytes and their precursors significantly retards postnatal oligodendrocyte growth and myelination. Our data indicate that IGF directly and specifically affects oligodendrocytes and myelination *in vivo* during development, and that IGF-IGF1R signaling in the cells of oligodendrocyte lineage is required for normal oligodendrocyte development and myelination. Our data also provide foundation for strategies to target IGF-IGF1R signaling pathway in oligodendrocyte lineage cells for treatment of demyelinating disorders. Whether IGF-IGF1R interaction promotes the growth of oligodendrocyte precursors and mature oligodendrocytes *in vivo* by utilizing the same intracellular molecular mechanisms, however, remains to be determined. Of notice, mice with blunted IGF1R expression in oligodendrocyte lineage cells maintain significant number of oligodendrocytes and myelination. Whether mechanism(s) that compensates loss of IGF1R exists also requires further investigation.

Acknowledgements

This work was supported by NIH grants RO1 NS038891 and RO1 NS048868. We thank Dr. Billie Moats-Staats for critic reading, Dr. Bill Stallcup for the NG2 antibody and Ms. Wei Pan, Haley Meyer and Rebecca Bigler for their technical assistance.

References

Abercrombie M. Estimation of nuclear population from microtome section. Anat Rec 1946;94:274–329.

Anlar B, Sullivan KA, Feldman EL. Insulin-like growth factor-I and central nervous system development. Horm Metab Res 1999;31:120–125. [PubMed: 10226791]

Araki K, Araki M, Miyazaki J, Vassalli P. Site-specific recombination of a transgene in fertilized eggs by transient expression of Cre recombinase. Proc Natl Acad Sci USA 1995;92:160–164. [PubMed: 7816809]

Ayer-LeLievre C, Stahlbom PA, Sara VR. Expression of IGF-I and -II mRNA in the brain and craniofacial region of the rat fetus. Development 1991;111:105–115. [PubMed: 2015788]

Bach MA, Shen-Orr Z, Lowe WL Jr, Roberts CT Jr, LeRoith D. Insulin-like growth factor I mRNA levels are developmentally regulated in specific regions of the rat brain. Brain Res Mol Brain Res 1996:48.

Baker J, Liu J-P, Robertson EJ, Efstratiadis A. Role of Insulin-like Growth Factors in embryonic and postnatal growth. Cell 1993;75:73–82. [PubMed: 8402902]

Barres BA, Hart IK, Coles HS, Burne JF, Voyvodic JT, Richardson WD, Raff MC. Cell death and control of cell survival in the oligodendrocyte lineage. Cell 1992;70:31–46. [PubMed: 1623522]

Barres BA, Jacobson MD, Schmid R, Sendnter M, Raff MC. Does oligodendrocyte survival depend on axons. Curr Biol 1993;3:489–497. [PubMed: 15335686]

Bartlett WP, Li X-S, Williams M. Expression of IGF-I mRNA in the murine subventricular zone during postnatal development. Mol Brain Res 1992;12:285–291. [PubMed: 1315903]

Bondy CA. Transient IGF-I gene expression during the maturation of functionally related central projection neurons. J Neurosci 1991;11:3442–3455. [PubMed: 1658250]

Bondy CA, Cheng CM. Signaling by insulin-like growth factor 1 in brain. Eur J Pharmacol 2004;490:25–31. [PubMed: 15094071]

Bondy CA, Werner H, Roberts CT Jr, LeRoith D. Cellular pattern of insulin-like growth factor-I (IGF-I) and type I IGF receptor gene expression in early organogenesis: Comparison with IGF-II gene expression. Mol Endocrinol 1990;4:1386–1398. [PubMed: 2172801]

Carson MJ, Behringer RR, Brinster RL, McMorris FA. Insulin-like growth factor I increases brain growth and central nervous system myelination in transgenic mice. Neuron 1993;10:729–740. [PubMed: 8386530]

Cheng CM, Joncas G, Reinhardt RR, Farrer R, Quarles R, Janssen J, McDonald MP, Crawley JN, Powell-Braxton L, Bondy C. Biochemical and morphometric analysis show that myelination in the insulin-like growth factor 1 null brain is proportionate to its neuronal composition. J Neurosci 1998;18:5673–5681. [PubMed: 9671658]

D'Ercole AJ, Ye P, Calikoglu AS, Gutierrez-Ospina G. The role of the insulin-like growth factors in the central nervous system. Mol Neurobiol 1996;13:227–255. [PubMed: 8989772]

Genoud S, Lappe-Siefke C, Goebbels S, Radtke F, Aguet M, Scherer SS, Suter U, Nave KA, Mantei N. Notch1 control of oligodendrocyte differentiation in the spinal cord. J Cell Biol 2002;158:709–718. [PubMed: 12186854]

Gregori N, Proschel C, Noble M, Mayer-Proschel M. The tripotential glial-restricted precursor (GRP) cell and glial development in the spinal cord: generation of bipotential oligodendrocyte-type-2 astrocyte progenitor cells and dorsal-ventral differences in GRP cell function. J Neurosci 2002;22:248–256. [PubMed: 11756508]

Herrera J, Yang H, Zhang SC, Proschel C, Tresco P, Duncan ID, Luskin M, Mayer-Proschel M. Embryonic-derived glial-restricted precursor cells (GRP cells) can differentiate into astrocytes and oligodendrocytes *in vivo*. Exp Neurol 2001;171:11–21. [PubMed: 11520117]

Hodge RD, D'Ercole AJ, O'Kusky JR. Insulin-like growth factor-I accelerates the cell cycle by decreasing G1 phase length and increases cell cycle reentry in the embryonic cerebral cortex. J Neurosci 2004;24:10201–10210. [PubMed: 15537892]

Hsieh J, Aimone JB, Kaspar BK, Kuwabara T, Nakashima K, Gage FH. IGF-1 instructs multipotent adult neural progenitor cells to become oligodendrocytes. J Cell Biol 2004;164:111–122. [PubMed: 14709544]

Ikenaka K, Kagawa T, Mikoshiba K. Selective expression of DM-20, an alternatively spliced myelin proteolipid protein gene product, in developing nervous system and in nonglial cells. J Neurochem 1992;58:2248–2253. [PubMed: 1374119]

Jakovcevski I, Zecevic N. Olig transcription factors are expressed in oligodendrocyte and neuronal cells in human fetal CNS. J Neurosci 2005;25:10064–10073. [PubMed: 16267213]

Jordan C, Friedrich V Jr, Dubois-Dalcq M. In situ hybridization analysis of myelin gene transcripts in developing mouse spinal cord. J Neurosci 1989;9:248–257. [PubMed: 2464047]

Klugmann M, Schwab MH, Puhlhofer A, Schneider A, Zimmermann F, Griffiths IR, Nave KA. Assembly of CNS myelin in the absence of proteolipid protein. Neuron 1997;18:59–70. [PubMed: 9010205]

Liu J-P, Baker J, Perkins AS, Robertson EJ, Efstratiadis A. Mice carrying null mutations of the genes encoding Insulin-like Growth Factor I (Igf-1) and type 1 IGF receptor. Cell 1993;75:59–72. [PubMed: 8402901]

Louvi A, Accili D, Efstratiadis A. Growth-promoting interaction of IGF-II with the insulin receptor during mouse embryonic development. Developmental Biology 1997;189:33–48. [PubMed: 9281335]

Lu QR, Yuk D, Alberta JA, Zhu Z, Pawlitzky I, Chen J, McMahon AP, Stiles CD, Rowitch DH. Sonic hedgehog-regulated oligodendrocyte lineage genes encoding bHLH proteins in the mammalian central nervous system. Neuron 2000;25:317–329. [PubMed: 10719888]

Lu QR, Sun T, Zhu ZM, Ma N, Garcia M, Stiles CD, Rowitch DH. Common developmental requirement for *Olig* function indicates a motor neuron/oligodendrocyte connection. Cell 2002;109:75–86. [PubMed: 11955448]

Luzi P, Zaka M, Rao HZ, Curtis M, Rafi MA, Wenger DA. Generation of transgenic mice expressing insulin-like growth factor-1 under the control of the myelin basic protein promoter: increased myelination and potential for studies on the effects of increased IGF-1 on experimentally and genetically induced demyelination. Neurochem Res 2004;29:881–889. [PubMed: 15139287]

Mason JL, Goldman JE. $A2B5^+$ and $O4^+$ cycling progenitors in the adult forebrain white matter respond differentially to PDGF-AA, FGF-2, and IGF-1. Mol Cell Neurosci 2002;20:30–42. [PubMed: 12056838]

Mason JL, Xuan S, Dragatsis I, Efstratiadis A, Goldman JE. Insulin-like growth factor (IGF) signaling through type 1 IGF receptor plays an important role in remyelination. J Neurosci 2003;23:7710–7718. [PubMed: 12930811]

Mason JL, Ye P, Suzuki K, D'Ercole AJ, Matsushima GK. Insulin-like growth factor-1 inhibits mature oligodendrocyte apoptosis during primary demyelination. J Neurosci 2000;20:5703–5708. [PubMed: 10908609]

Masters BA, Werner H, Roberts CT Jr, LeRoith D, Raizada MK. Insulin-like growth factor I (IGF-I) receptors and IGF-I action in oligodendrocytes from rat brains. Regulatory Peptides 1991;33:117–131. [PubMed: 1652776]

McMorris FA, Dubois-Dalcq M. Insulin-like growth factor I promotes cell proliferation and oligodendroglial commitment in rat glial progenitor cells developing in vitro. J Neurosci Res 1988;21:199–209. [PubMed: 3216421]

McMorris FA, Mozell RL, Carson MJ, Shinar Y, Meyer RD, Marchetti N. Regulation of oligodendrocyte development and central nervous system myelination by insulin-like growth factors. [Review]. Ann NY Acad Sci 1993;692:321–334. [PubMed: 8215042]

McMorris FA, Smith TM, DeSalvo S, Furlanetto RW. Insulin-like growth factor I/somatomedin C: a potent inducer of oligodendrocyte development. Proc Natl Acad Sci USA 1986;83:822–826. [PubMed: 3511475]

Mercer EH, Hoyle GW, Kapur RP, Brinster RL, Palmiter RD. The dopamine P-hydroxylase gene promoter directs expression of E. Coli LacZ to sympathetic and other neurons in adult transgenic mice. Neuron 1991;7:703–716. [PubMed: 1742021]

Milner RJ, Lai C, Nave KA, Lenoir D, Ogata J, Sutcliffe JG. Nucleotide sequences of two mRNAs for rat brain myelin proteolipid protein. Cell 1985;42:931–939. [PubMed: 2414013]

Mozell RL, McMorris FA. Insulin-like growth factor I stimulates oligodendrocyte development and myelination in rat brain aggregate cultures. J Neurosci Res 1991;30:382–390. [PubMed: 1665869]

Nave KA, Milner RJ. Proteolipid proteins: structure and genetic expression in normal and myelin-deficient mutant mice. [Review]. Critical Rev Neurobiol 1989;5:65–91. [PubMed: 2670252]

Ni W, Rajkumar K, Nagy JI, Murphy LJ. Inpaired brain development and reduced astrocyte response to injury in transgenic mice expressing IGF binding protein-1. Brain Res 1997;769:97–107. [PubMed: 9374277]

Popken GJ, Dechert-Zeger M, Ye P, D'Ercole AJ. Brain development. Adv Exp Med Biol 2005;567:187–220. [PubMed: 16372399]

Rao MS, Noble M, Mayer-Proschel M. A tripotential glial precursor cell is present in the developing spinal cord. Proc Natl Acad Sci USA 1998;95:3996–4001. [PubMed: 9520481]

Saneto RP, Low KG, Melner MH, De Vellis J. Insulin/insulin-like growth factor I and other epigenetic modulators of myelin basic protein expression in isolated oligodendrocyte progenitor cells. J Neurosci Res 1988;21:210–219. [PubMed: 2464075]

Shiota C, Miura M, Mikoshiba K. Developmental profile and differential localization of mRNAs of myelin proteins (MBP and PLP) in oligodendrocytes in the brain and in culture. Brain Res Dev Brain Res 1989;45:83–94.

Sidman, RL.; Abervine, JB.; Pierec, ET. Altas of the mouse brain and spinal cord. Cambridge, MA: Harvard University Press; 1971.

Sorg BA, Smith MM, Campagnoni AT. Developmental expression of the myelin proteolipid protein and basic protein mRNAs in normal and dysmyelinating mutant mice. J Neurochem 1987;49:1146–1154. [PubMed: 2442307]

Spassky N, Olivier C, Perez-Villegas E, Goujet-Zalc C, Martinez S, Thomas J, Zalc B. Single or multiple oligodendroglial lineages: a controversy. [Review] [19 refs]. GLIA 2000;29:143–148. [PubMed: 10625332]

Werner H, Woloschhak M, Adamo M, Shen-Orr, Brberts CT Jr, LeRoith D. Developmental regulation of the rat insulin-like growth factor I receptor gene. Proc Natl Acad Sci USA 1989;86:7451–7455. [PubMed: 2477843]

Xuan S, Kitamura T, Nakae J, Politi K, Kido Y, Fisher PE, Morroni M, Cinti S, White MF, Herrera PL, Accili D, Efstratiadis A. Defective insulin secretion in pancreatic beta cells lacking type 1 IGF receptor. J Clin Invest 2002;110:1011–1019. [PubMed: 12370279]

Ye P, Carson J, D'Ercole AJ. In vivo actions of insulin-like growth factor-I (IGF-I) on brain myelination: studies of IGF-I and IGF binding protein-1 (IGFBP-1) transgenic mice. Journal of Neuroscience 1995a;15:7344–7356. [PubMed: 7472488]

Ye P, Carson J, D'Ercole AJ. Insulin-like growth factor-I influences the initiation of myelination: studies of the anterior commissure of transgenic mice. Neurosci Lett 1995b;201:235–238. [PubMed: 8786848]

Ye P, D'Ercole AJ. Insulin-like growth factor I protects oligodendrocytes from tumor necrosis factor-α-induced injury. Endocrinology 1999;140:3063–3072. [PubMed: 10385398]

Ye P, D'Ercole AJ. Insulin-like growth factor actions during development of neural stem cells and progenitors in the central nervous system. J Neurosci Res 2006;83:1–6. [PubMed: 16294334]

Ye P, Lee K-H, D'Ercole AJ. Insulin-like growth factor-I (IGF-I) protects myelination from undernutritional insult: Studies of transgenic mice overexpressing IGF-I in brain. J Neurosci Res 2000;62:700–708. [PubMed: 11104508]

Ye P, Li L, Richards RG, DiAugustine RP, D'Ercole AJ. Myelination is altered in insulin-like growth factor-I null mutant mice. J Neurosci 2002;22:6041–6051. [PubMed: 12122065]

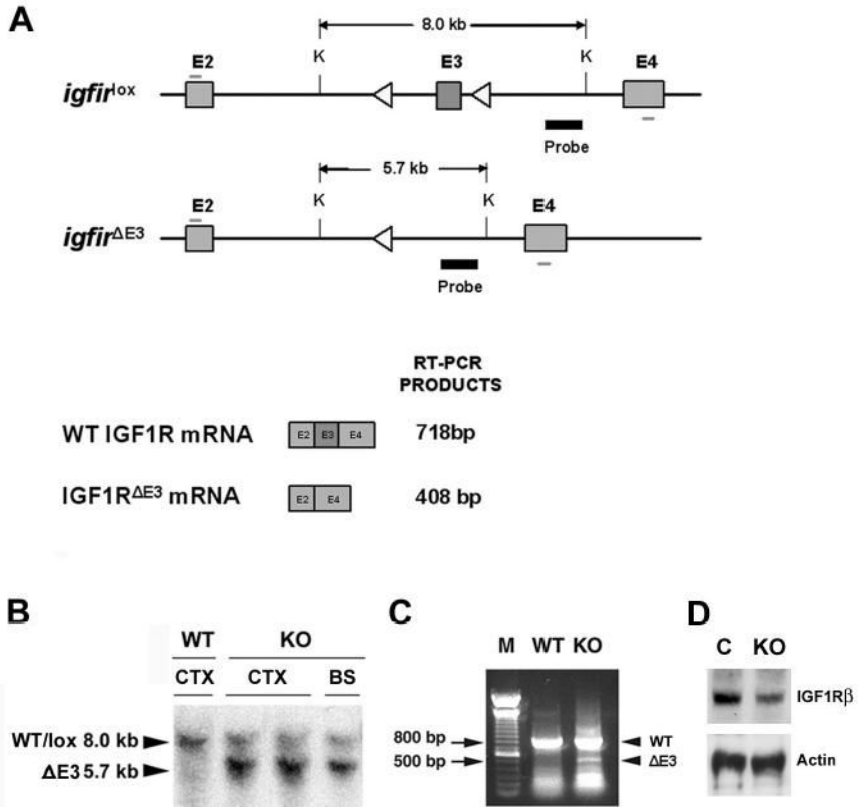

Figure 1.

Schematic diagram of mutant *igf1r* genes, and representative genotype analyses of conditional *igf1r* mutant (KO) and wildtype (WT) mice. ***Panel A***. Schematic diagram of mutant *igf1r* genes with loxed or deleted E3 (upper diagrams) and their mRNAs (lower diagrams). The exons of loxed (*igf1r*^{lox}) or E3-deleted (*igf1r* ^{E3}) *igf1r* genes are represented by shaded boxes and their number labeled above each exon. Lox sequences were represented by open triangles. The position of a DNA probe used for Southern blot analysis is indicated by a thick black line, and the primers for RT-PCR are indicated by the short thin lines above E2 and below E4. The size of the Southern blot-detected Kpn I (K)-digested DNA fragment in *igf1r*^{lox} and E3 *igf1r* ^{E3} gene is indicated above the DNA fragment. The schematic diagram is not drawn to scale. ***Panel B***. Representative Southern blot analysis of brain genomic DNA from a 2-week-old IGF1R$^{pre\text{-}oligo\text{-}ko}$ mouse and a WT mouse. The sizes of DNA bands detected are indicated by two arrowheads at the left side of the image. CTX = cerebral cortex; BS = brainstem. ***Panel C***. Representative RT-PCR analysis of mRNA isolated from CTX of a 2-week-old IGF1R$^{oligo\text{-}ko}$ mouse and a WT mouse. DNA ladder markers (M) were loaded on the left side of the gel, and 500 and 800 base pair (bp) bands are indicated by two arrows. Note that the bands at the bottom of both WT and KO lanes are DNA primer dimers. ***Panel D.*** A representative Western immunoblot showing the abundance of the IGF1R-β subunit in whole brain of a newborn IGF1R$^{pre\text{-}oligo\text{-}ko}$ mouse (KO) and a control mouse (C).

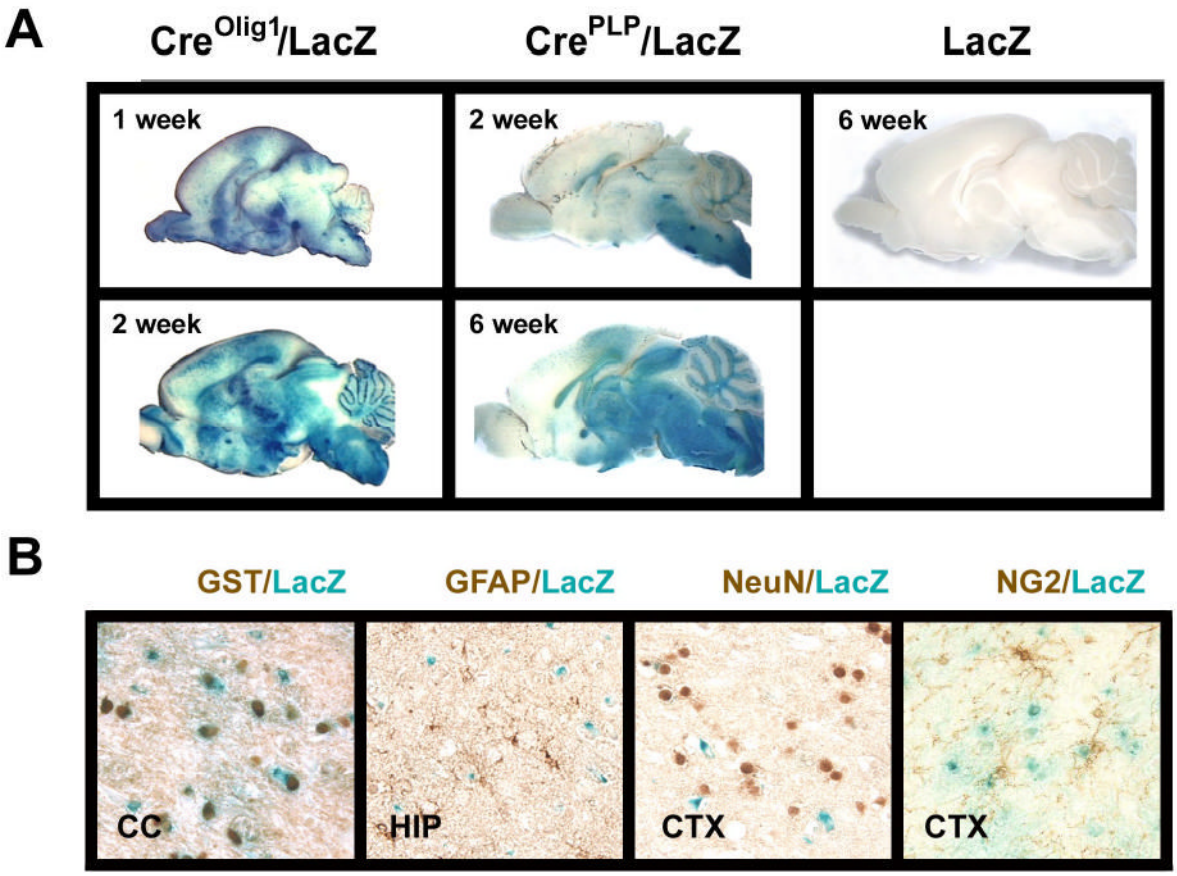

Figure 2.

Developmental (panel A) and cellular (panels B) expression pattern of Cre^{Olig1} and Cre^{PLP} transgenes. ***Panel A***. Brains of $Cre^{Olig1}/LacZ^{actin\text{-}stop}$ (left two panels) and $Cre^{PLP}/LacZ^{actin\text{-}stop}$ (middle two panels) double Tg mice, as well as a $LacZ^{actin\text{-}stop}$ Tg mouse (right panel), at postnatal age of 1 week, 2 weeks, or 6 weeks, were subjected to LacZ histochemical staining. The 6-week-old $LacZ^{actin\text{-}stop}$ Tg mouse exhibited no LacZ staining. ***Panel B***. LacZ and immunohischemical double-staining of brain sections of 4-week-old $Cre^{PLP}/LacZ^{actin\text{-}stop}$ mice. CC= corpus callsoum, HIP=hippocampus, and CTX = cerebral cortex.

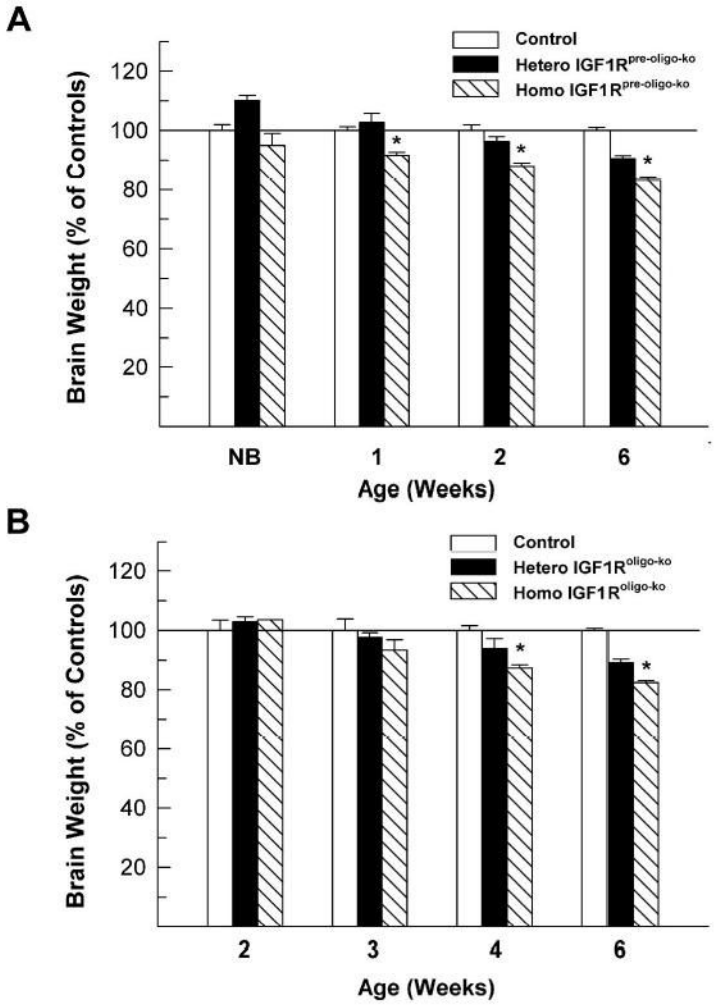

Figure 3.

Brain weights of IGF1R$^{pre\text{-}oligo\text{-}ko}$ (panel A) and IGF1R$^{oligo\text{-}ko}$ (panel B) mutant mice during development. Brain weight is expressed as percentage of controls, and values are means ± SE from 6 -10 mice. A line is drawn at 100% to facilitate comparison. NB = newborn. *, $P < 0.01$, compared to WT.

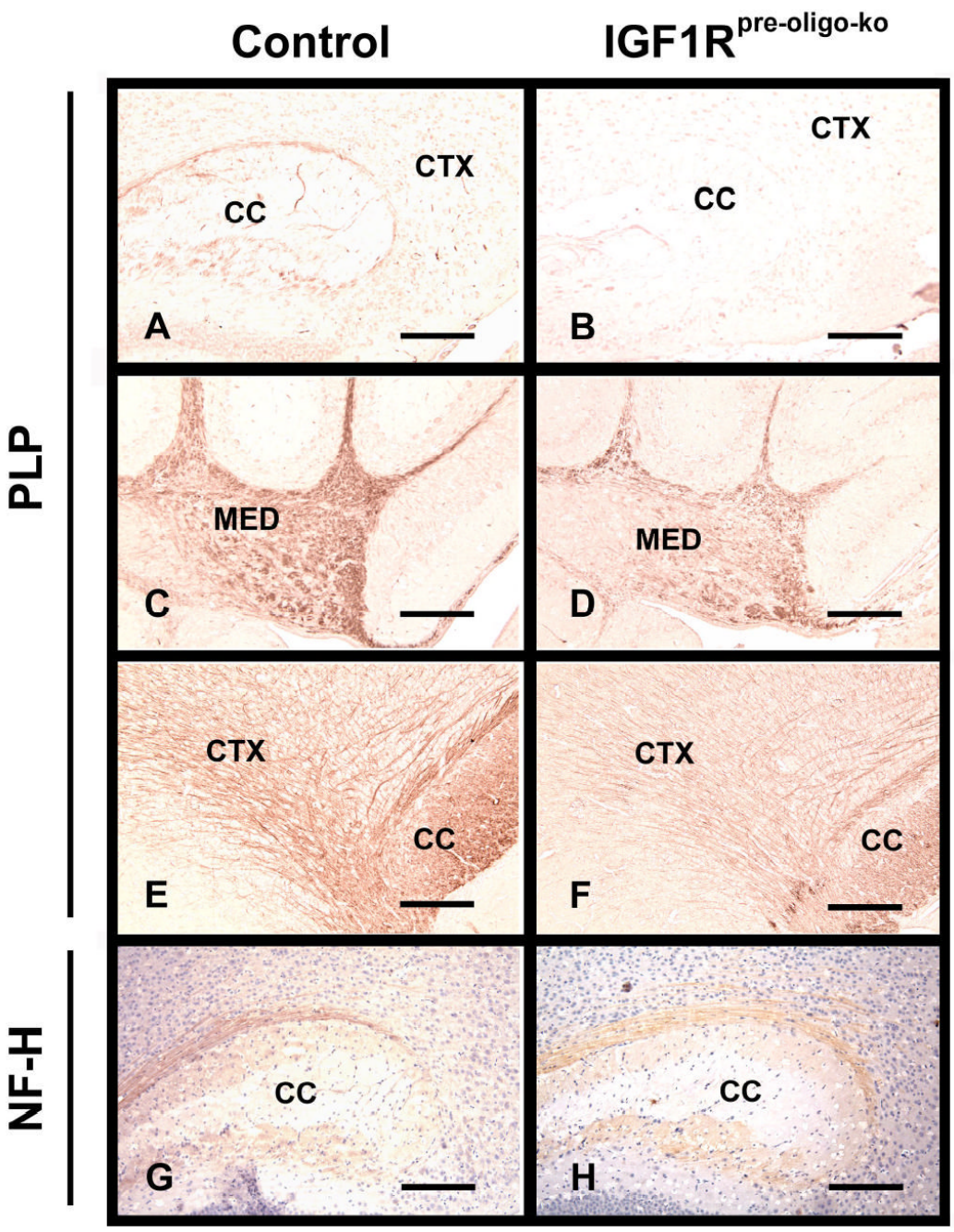

Figure 4.

PLP and NF-H immunostaining in brains of IGF1R$^{pre\text{-}oligo\text{-}ko}$ mice (panels B, D, F and H) and their littermate controls (panels A, C, E and G). Brains from 2-week-old (panels A, B, C, D, G and H) and 6-week-old (panels E and F) IGF1R$^{pre\text{-}oligo\text{-}ko}$ mice and their littermate controls were stained with PLP antibody (panels A, B, C, D, E and F) or NF-H antibody (panels G and H). After NF-H immunostaining, sections were counterstained with hematoxylin. CTX = cerebral cortex, CC = corpus callosum, and MED = cerebellar medulla. The scale bar represents 200 μm in panels A, B, C, D, G and H, and 100 μm in E and F, respectively.

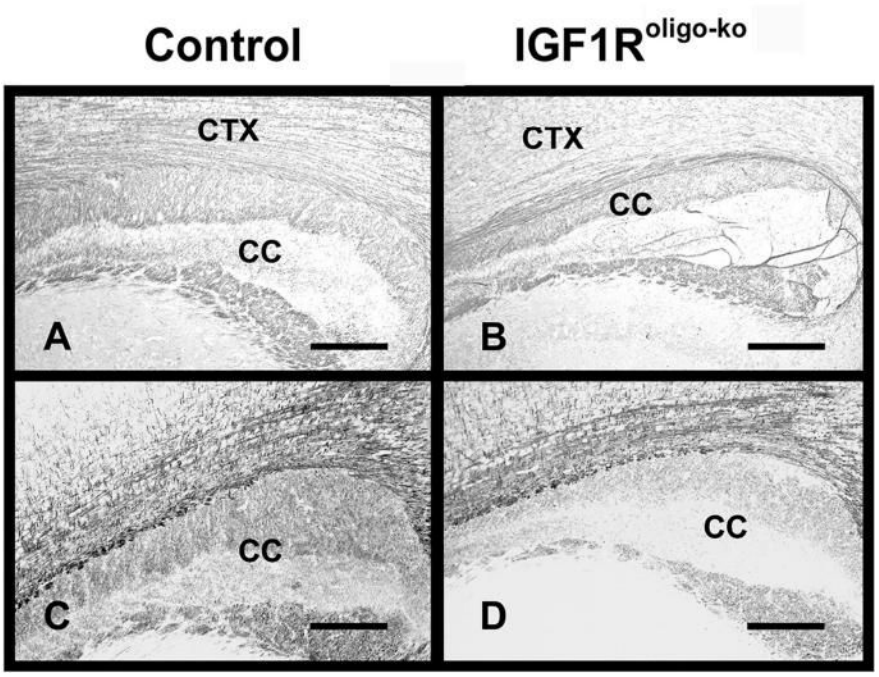

Figure 5.

PLP immunostaining brains of IGF1R$^{oligo\text{-}ko}$ mice and their littermate controls. Brains from IGF1R$^{oligo\text{-}ko}$ mice (panels B and D) and their littermate controls (panels A and C) at 4 weeks (panels A and B) or 25 weeks (panels C and D) of age were stained with PLP antibody. CTX = cerebral cortex, and CC = corpus callosum. The scale bar represents 200 μm.

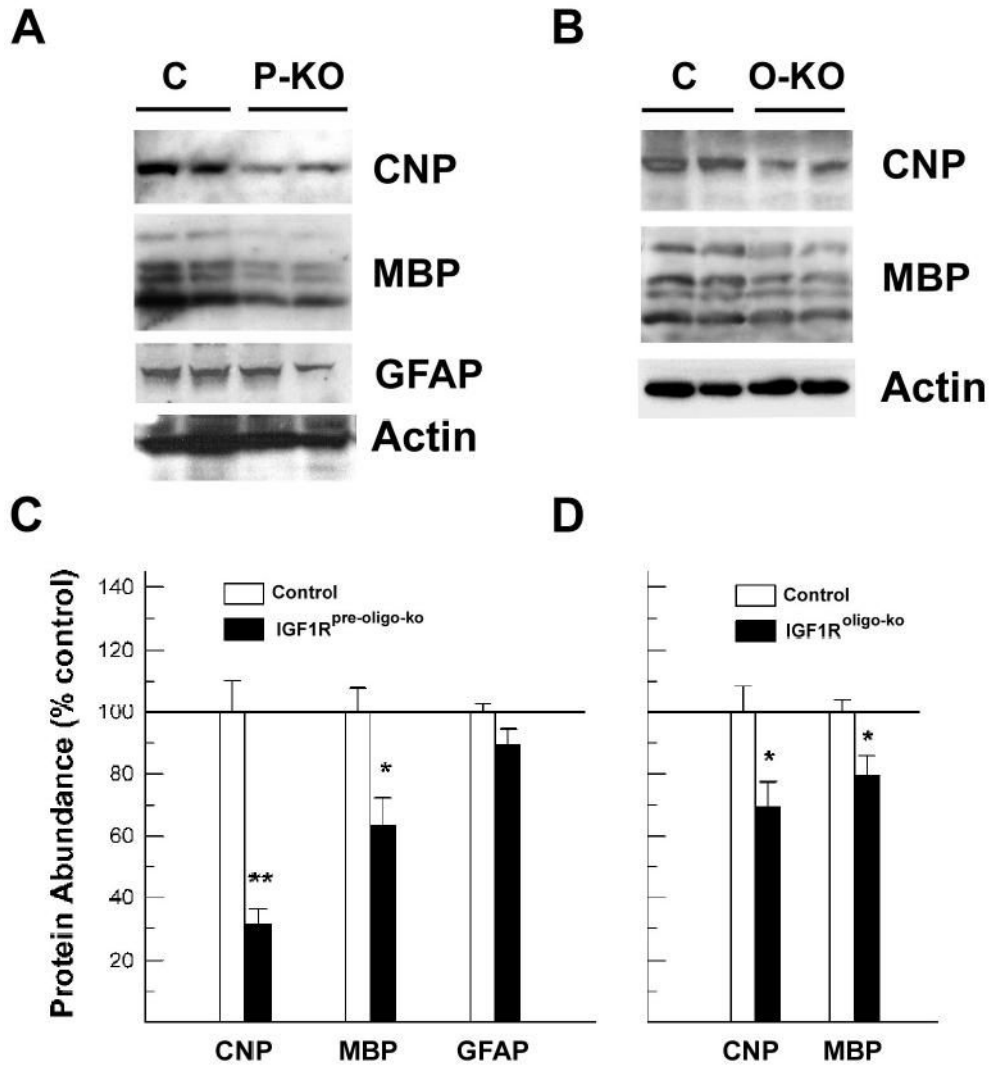

Figure 6.

Western immunoblot analysis of CNP, MBP and GFAP in the cerebral cortex of IGF1R$^{pre\text{-}oligo\text{-}ko}$ and IGF1R$^{oligo\text{-}ko}$ mice. ***Panel A.*** Representative Western immunoblot of CNP, MBP and GFAP protein in 2-week-old IGF1R$^{pre\text{-}oligo\text{-}ko}$ (P-KO) mice and controls (C). ***Panel B.*** Representative Western immunoblot of CNP and MBP protein in 6-week-old IGF1R$^{oligo\text{-}ko}$ (O-KO) mice and littermate controls (C). ***Panel C.*** Quantitative analysis of CNP, MBP and GFAP protein abundance in 2-week-old IGF1R$^{pre\text{-}oligo\text{-}ko}$ mice. ***Panel D.*** Quantitative analysis of CNP and MBP protein abundance in 6-week-old IGF1R$^{oligo\text{-}ko}$ mice. The protein abundance is expressed as percentage of that in controls, and values are mean ± SE of 3 –5 samples. A line is drawn at 100% to facilitate comparison. *, $P < 0.05$; **, $P < 0.01$, compared to controls.

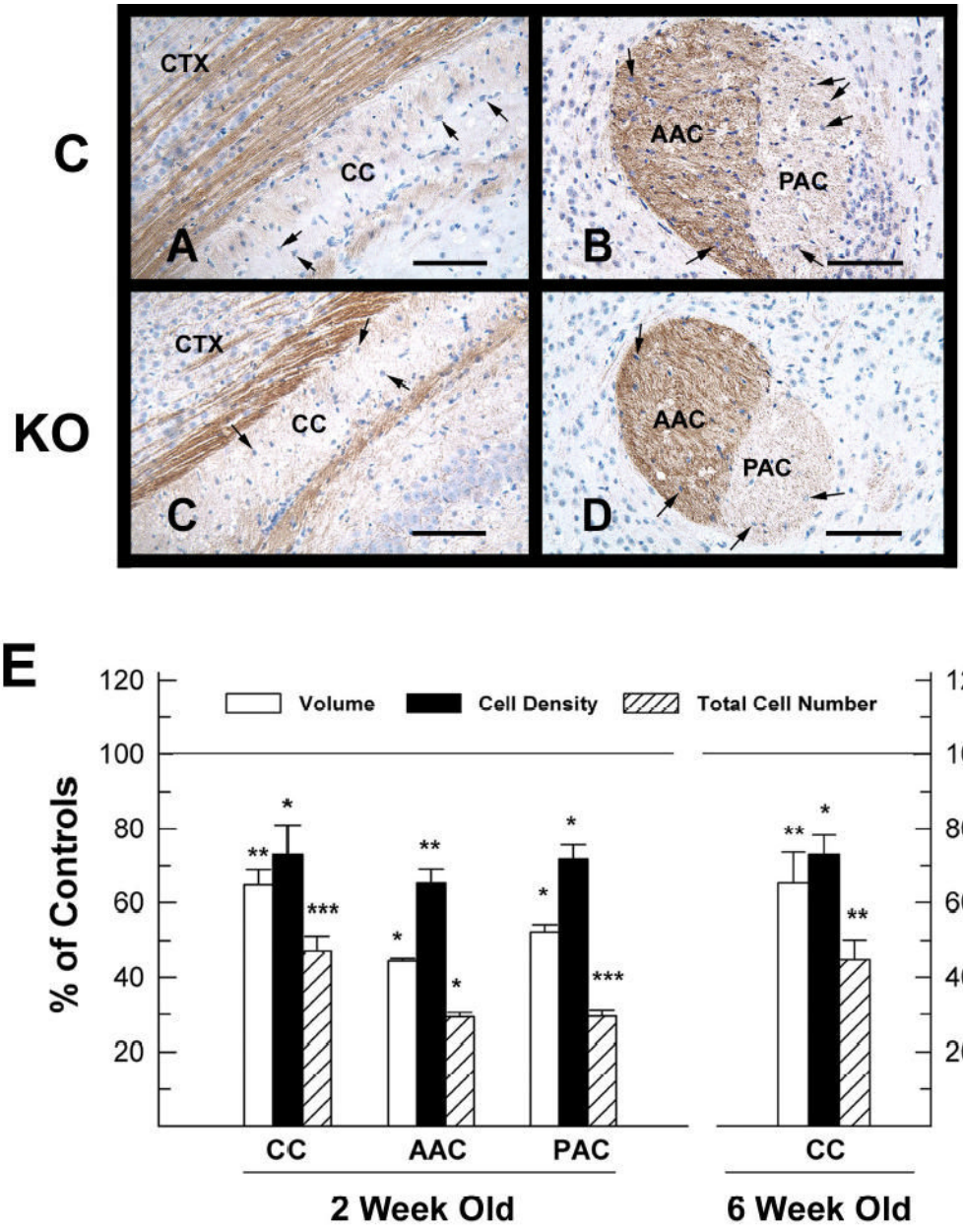

Figure 7.

Volume, cell density and cell number in corpus callosum (CC) and anterior commissure (AC) of 2-week-old IGF1R$^{pre\text{-}oligo\text{-}ko}$ mice and their littermate controls. ***Panels A-D.*** Representative photomicrographs of NF-H immunostained CC (panels A and C) and AC (panels B and D) from an IGF1R$^{pre\text{-}oligo\text{-}ko}$ mutant (panels C and D) and a control (panels A and B) mouse. Note that the number of purple/blue-stained cell nuclei is significantly decreased in the CC, anterior (AAC) and posterior (PAC) portions of AC of the IGF1R$^{pre\text{-}oligo\text{-}ko}$ mouse. CTX= cerebral cortex and HIP = hippocampus. The scale bars = 100 μm. ***Panel E***. Quantification of the volume, cell density and total number of cells in CC and AC. Values are expressed as percentage of control, and represent mean ± SE of 3 –6 samples. *, $P < 0.05$; **, $P < 0.01$; and ***, $P< 0.001$, compared to controls.

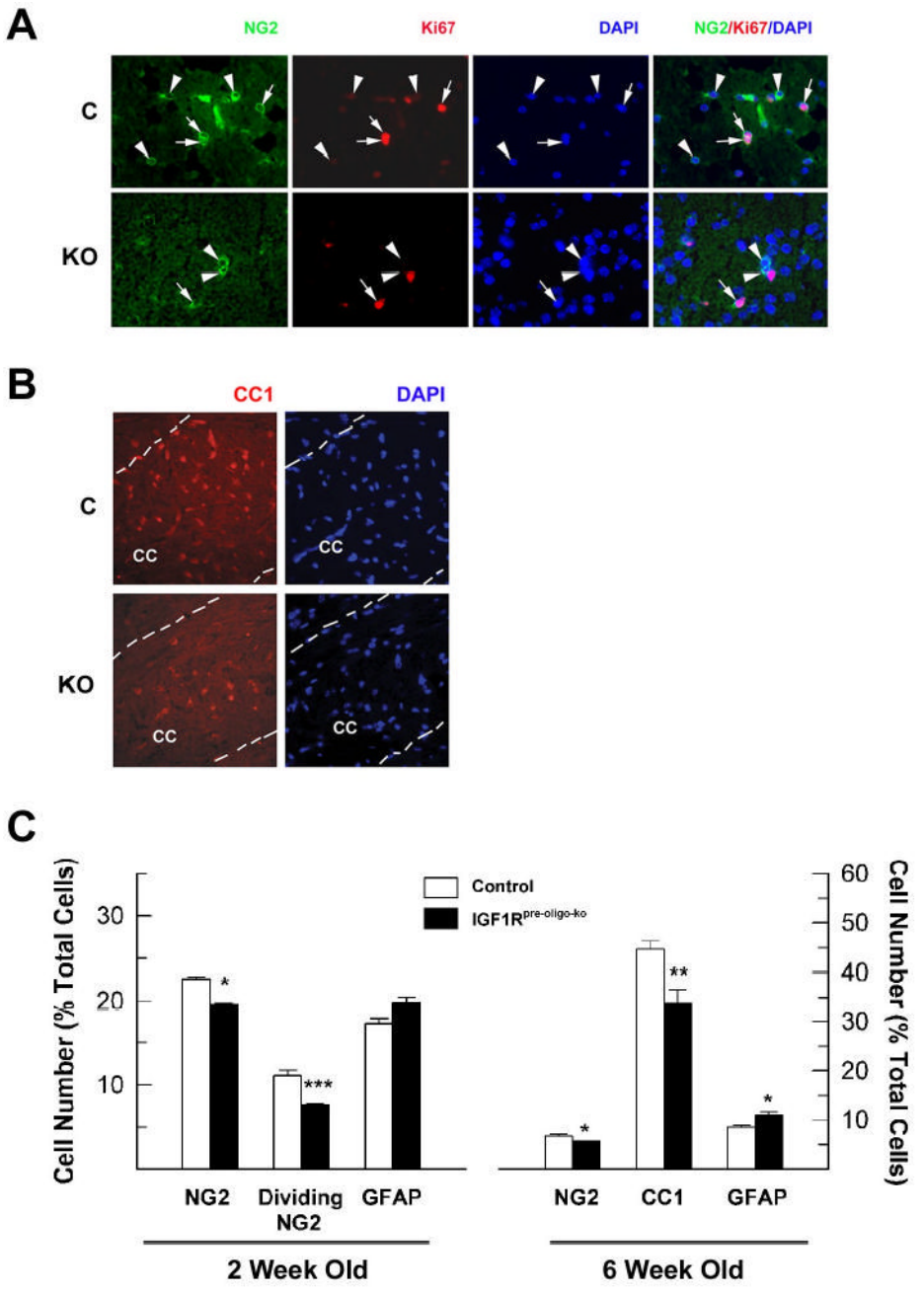

Figure 8.

The number of NG2$^+$ oligodendrocyte precursors, CC1$^+$ oligodendrocytes and GFAP$^+$ astrocytes in the CC of IGF1R$^{pre\text{-}oligo\text{-}ko}$ mutant (KO) and their littermate controls (C). ***Panel A***. Representative photomicrographs of double NG2 and Ki67 immunostaining from a 2-week-old IGF1R$^{pre\text{-}oligo\text{-}ko}$ and a control mouse. Arrowheads indicate NG2$^+$ precursors, and arrows point to cells positive for both NG2 and Ki67. Photomicrographs of merged NG2, Ki67, and DAPI images are shown in the right column. NG2 and Ki67 double-labeled cells are more numerous in the control brain. ***Panel B***. Representative photomicrographs of CC1 immunostaining of CC from a 6-week-old IGF1R$^{pre\text{-}oligo\text{-}ko}$ mutant mouse and a littermate control mouse. Dotted lines outline the CC. ***Panel C***. Quantification of NG2$^+$, proliferating NG2$^+$, CC1$^+$ and GFAP$^+$ cells in the CC of IGF1R$^{pre\text{-}oligo\text{-}ko}$ mice at 2 and 6 weeks of age.

Values represent mean ± SE of 3 – 4 mice from each group. *, $P < 0.05$; **, $P < 0.02$; ***, $P < 0.01$; compared to controls.

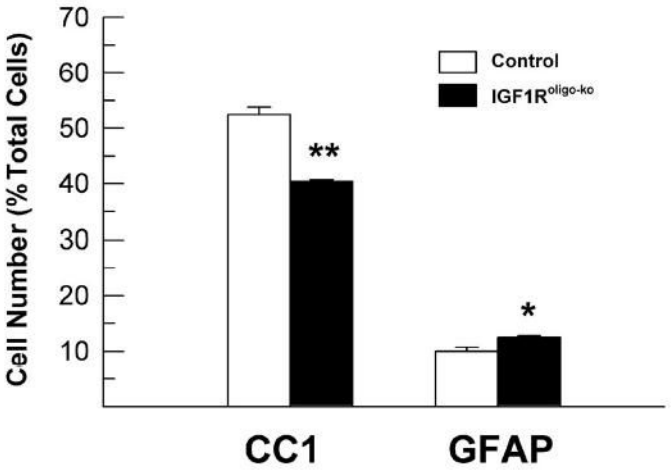

Figure 9.

The number of $CC1^+$ and $GFAP^+$ cells in the CC of $IGF1R^{oligo\text{-}ko}$ mice at 25 weeks of age. Values represent mean ± SE of 3 - 4 mice from each group. *, $P < 0.05$; **, $P < 0.001$, compared to controls.

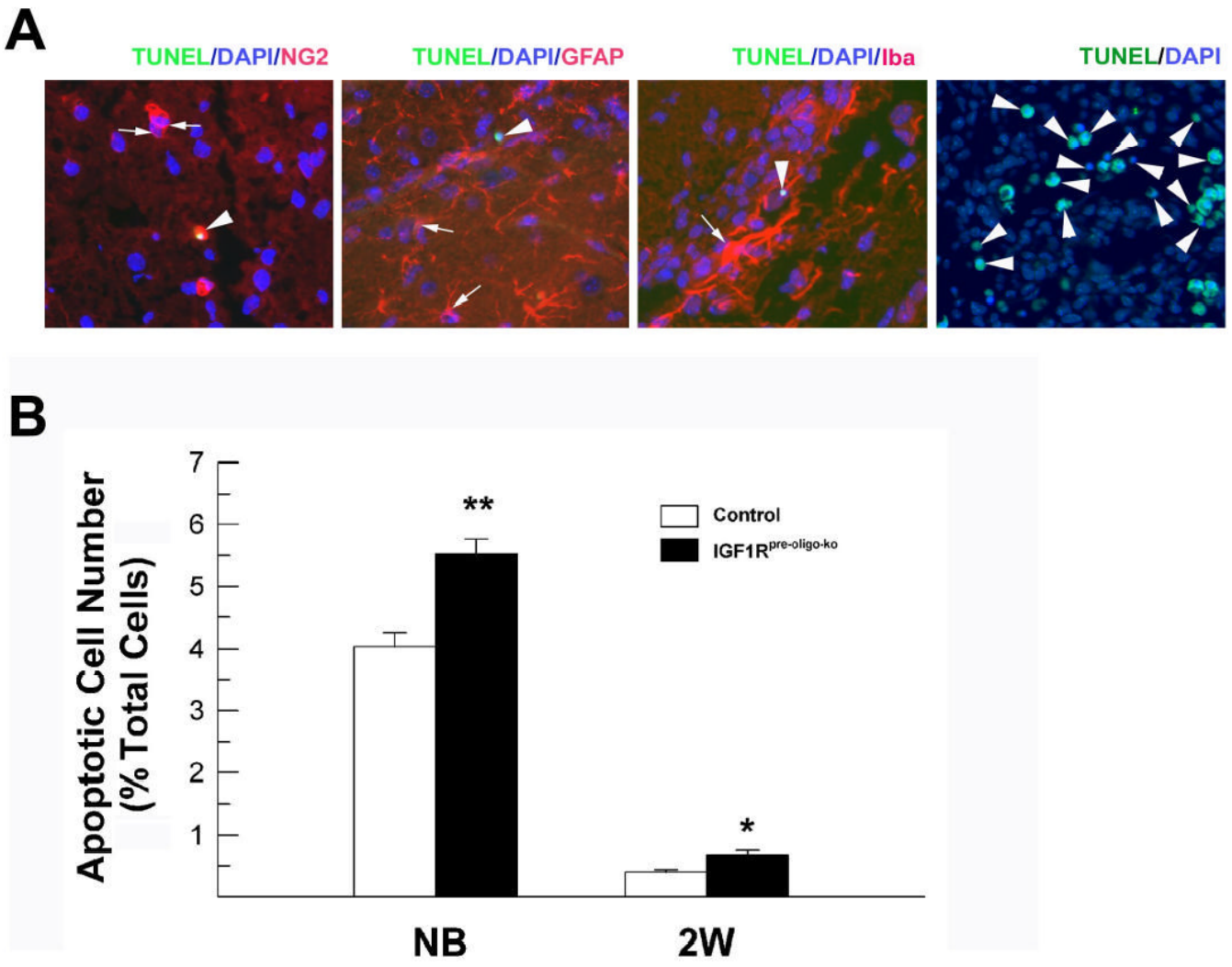

Figure 10.

Apoptotic cells in the CC of IGF1R$^{pre\text{-}oligo\text{-}ko}$ mice and their littermates. ***Panel A***. Representative photomicrographs of double TUNEL staining and NG2, GFAP, or Iba-1 immunostaining in the CC of an IGF1R$^{pre\text{-}oligo\text{-}ko}$ mouse at 2 weeks of age. A section from an E16 rat paw was used as a positive control for TUNEL staining (right panel). Arrowheads in each panel indicate TUNEL-labeled apoptotic cells. Arrows point to NG2^{+}, GFAP^{+} and Iba-1^{+} cells, respectively, in the left three panels. Note that in the left-most panel an arrowhead points to a TUNEL and NG2 double-labeled cell. ***Panel B***. Quantification of apoptotic cells in the CC of newborn and 2-week-old IGF1R$^{pre\text{-}oligo\text{-}ko}$ mice and their controls. Values represent mean ± SE of 3 - 4 mice from each group. *, $P < 0.05$; **, $P < 0.01$, compared to controls.

Table 1

Corpus callosum (CC) volume, cell density and total cell number in IGF1R$^{oligo\text{-}ko}$ mice and their littermate controls at 25 weeks of age.

	Control	KO	Change
CC volume (mm^3)	3.12 ± 0.18	2.40 ± 0.08 *	⇓ ~23%
Cell density (×1,000/mm^3)	307.99 ± 7.44	282.78 ± 5.57	⇓ ~ 8%
Total cell number (×1,000)	962.92 ± 75.83	680.12 ± 34.29 *	⇓ ~29%

Values represent mean ± SE of 3 mice from each group.

*, $P < 0.05$, compared to controls.

Table 2

Volume of dentate gyrus (DG) and granule cell layer (GCL), and total granule cell (GC) number in 2-week-old IGF1R$^{pre\text{-}oligo\text{-}ko}$ mice (KO) and their littermate controls.

	Controls	KO
DG Volume (mm^3)	4.58 ± 0.13	3.35 ± 0.20 *
GCL Volume (mm^3)	1.15 ± 0.04	0.83 ± 0.05 *
Total GC number (×1,000)	940.66 ± 25.58	830.10 ± 38.14

Values represent mean ± SE of 3 - 4 mice from each group.

*, $P < 0.01$, compared to controls.